

Article

London Dispersive and Lewis Acid-Base Surface Energy of 2D Single-Crystalline and Polycrystalline Covalent Organic Frameworks

Tayssir Hamieh ^{1,2} 

¹ Faculty of Science and Engineering, Maastricht University, P.O. Box 616, 6200 MD Maastricht, The Netherlands; t.hamieh@maastrichtuniversity.nl

² Laboratory of Materials, Catalysis, Environment and Analytical Methods Laboratory (MCEMA), Faculty of Sciences, Lebanese University, Hadath, Badaro, Beirut P.O. Box 6573/14, Lebanon

Abstract: This paper is devoted to an accurate determination of the London dispersive, polar free energy of adsorption, Lewis acid γ_s^+ and Lewis base γ_s^- components of the polar surface energy γ_s^{AB} of 2D single-crystalline and polycrystalline covalent organic frameworks such as TAPPy-TPA-COFs. The obtained results showed the highest values of polar and total surface energy of the polycrystalline COF relative to those of the single-crystalline COF. Inverse gas chromatography (IGC) at infinite dilution was used to quantify the various surface parameters of the different materials. The net retention times of the adsorption of n-alkanes and several polar solvents on single-crystalline and polycrystalline covalent organic frameworks were obtained from IGC measurements. The free surface Gibbs energy of adsorption was obtained for the various organic molecules at different temperatures from their net retention volume values. The separation between the London dispersive energy and the polar energy of adsorbed molecules was carried out by using a new thermodynamic parameter \mathcal{P}_{SX} chosen as new indicator variable and taking into account the deformation polarizability and the harmonic mean of the ionization energies of solvents and solid materials, derived from the London dispersion equation. The obtained results gave higher acidity ($K_A = 0.22$) for the 2D polycrystalline COF than that of the single-crystalline COF ($K_A = 0.15$) and an equivalent basicity of the two COFs. The obtained results are very promising for the accurate determination of the surface thermodynamic parameters of adsorption of organic solvents on solid surfaces.



Citation: Hamieh, T. London Dispersive and Lewis Acid-Base Surface Energy of 2D Single-Crystalline and Polycrystalline Covalent Organic Frameworks. *Crystals* **2024**, *14*, 148. <https://doi.org/10.3390/cryst14020148>

Academic Editors: Aurelia Visa and Rosario Mercedes Pérez Colodrero

Received: 18 January 2024

Revised: 27 January 2024

Accepted: 28 January 2024

Published: 31 January 2024



Copyright: © 2024 by the author. Licensee MDPI, Basel, Switzerland. This article is an open access article distributed under the terms and conditions of the Creative Commons Attribution (CC BY) license (<https://creativecommons.org/licenses/by/4.0/>).

Keywords: deformation polarizability; ionization energy; London dispersive free energy; polar energy of adsorption; Lewis acid–base components of surface energy; molecular separation distance

1. Introduction

Covalent organic frameworks (COFs), discovered in 2005 [1], are very interesting crystalline organic porous materials exhibiting very important surface properties concerning their large specific surface area and porosity [2]. Many research projects on COFs and their synthesis were developed, due to their suitability to be used as excellent materials in various applications such as catalysis [3–7], rechargeable batteries [8–10], separation processes [11], light-emitting materials [12], biomedicine, biosensors and bioelectronics [13,14].

Some promising covalent organic frameworks, such as 2D COFs composed of layered 2D polymers, exhibited excellent thermal conductivity [15] and heterogeneous catalytic activity [16]. Two-dimensional imine-based covalent organic frameworks, such as single-crystalline (SC) and polycrystalline TAPPy-TPA-COF (PC) (Figure 1) synthesized from 4,4',4'',4'''-(pyrene-1,3,6,8-tetrayl) tetraaniline (TAPPy) and terephthalaldehyde (TPA), were recently studied by several authors [17–22]. The physicochemical properties of 2D COFs were studied by inverse gas chromatography at infinite dilution by Natraj et al. [18] and Yusuf et al. [19].

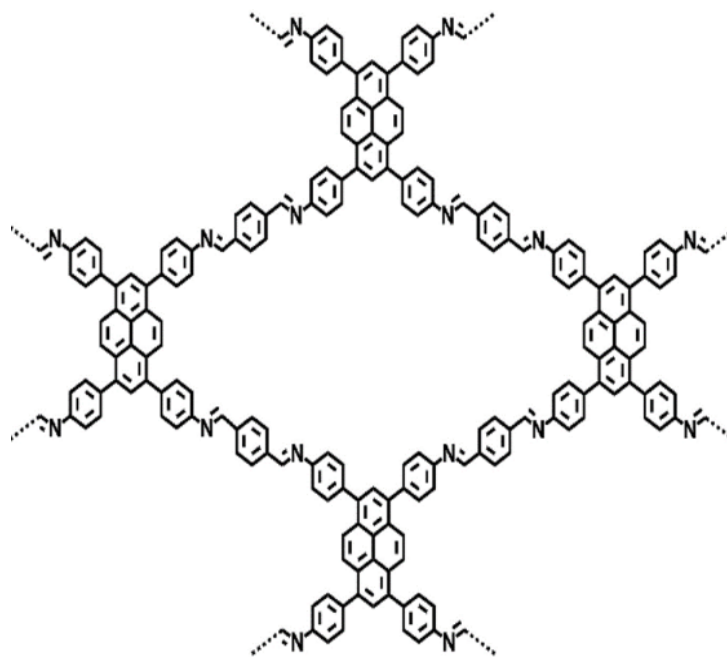


Figure 1. Chemical structure of TAPPy-TPA-COF.

This paper is devoted to determining the London dispersive, polar free energy, Lewis acid γ_s^+ and Lewis base γ_s^- components of polar surface energy γ_s^{AB} of 2D single-crystalline and polycrystalline covalent organic frameworks such as TAPPy-TPA-COFs. The used technique was inverse gas chromatography (IGC) at infinite dilution [23–40] based on the experimental determination of the net retention time t_n and volume V_n of several organic molecules adsorbed on the solid materials. The fundamental thermodynamic equation of IGC allowed for the calculation of the free energy of adsorption ΔG_a^0 of any organic solvents on a solid surface, given in infinite dilution by Equation (1):

$$\Delta G_a^0 = -RT \ln V_n + RT \ln \left(\frac{sm\pi_0}{P_0} \right) \quad (1)$$

where T is the absolute temperature of the chromatographic column containing the solid material, R the perfect gas constant, m the mass of the solid material of a specific surface area s , and π_0 and P_0 are two reference characteristics referred to as the two-dimensional state and atmospheric pressure, respectively.

In the case of non-polar solvents such as n-alkanes, the only free energy of adsorption is that of the London dispersion component ΔG_a^d given by the following:

$$\Delta G_a^0 = \Delta G_a^d \quad (2)$$

For polar organic molecules, the specific free energy ΔG_a^{sp} of adsorption has to be added following Equation (3):

$$\Delta G_a^0 = \Delta G_a^d + \Delta G_a^{sp} \quad (3)$$

Many methods and models have been proposed in the literature [23–33] to determine the ΔG_a^{sp} of polar solvents adsorbed on solid materials and the London dispersive surface energy γ_s^d of the studied materials. These chromatographic methods used the linearity of ΔG_a^0 or $RT \ln V_n$ of n-alkanes (from n-pentane to n-decane) adsorbed on a solid surface as a function of a chosen thermodynamic parameter at different temperatures. The separation between the dispersive and specific free energy of adsorption was based on the use of polar organic molecules such as dichloromethane, chloroform, tetrachloromethane, benzene, acetone, toluene, ethyl acetate, diethyl ether, etc. The boiling point $T_{B.P.}$ of organic solvents [30] was first used to study the surface properties of solid materials. Next, a method based

on the vapor pressure P_0 of the solvents was proposed [23–25] to separate the dispersive and specific components of the free surface energy. This most popular method was then followed by another one that used the dispersive component γ_1^d of the surface energy of the probes [26]. Later, the deformation polarizability α_0 [27] was introduced to solve the same problem consisting in the determination of the specific energy of adsorption. Next, the standard enthalpy of vaporization ΔH_{vap}^0 [31] was proposed. The topological index χ_T [28,29] was then used to evaluate the specific interactions between solids and organic molecules.

The values of ΔG_a^{sp} and γ_s^d obtained by the various chromatographic methods are very different and strongly depend on the molecular model and IGC method used. In previous papers, it was shown that the surface area of organic molecules not only depends on the chosen surface areas of molecules but also on the temperature [32–36], and this certainly affects the different surface thermodynamic parameters. On the other hand, the proposed expressions of the surface areas of organic molecules leading to the correction of γ_s^d of solids cannot be always transferred to any other solid.

In a recent paper [41], a new method based on the London dispersion expression [42] was proposed by using a new thermodynamic parameter \mathcal{P}_{SX} dependent both on the deformation polarizability α_{0X} of the probe and on the ionization energies of the solid ε_S and the solvent ε_X :

$$\mathcal{P}_{SX} = \frac{\varepsilon_S \varepsilon_X}{(\varepsilon_S + \varepsilon_X)} \alpha_{0X} \quad (4)$$

This new method constituted a correction of Donnet et al.'s method that used the concept of the deformation polarizability of molecules. The proposed method took into consideration all physicochemical parameters intervening in the London equation [42] that were neglected in the approach of Donnet et al. [27]. This method, based on the equation of the London dispersion interaction [42], was used to better quantify the different Lewis acid–base contributions to the surface energy of single-crystalline and polycrystalline COFs as well as their polar surface energy. By using this new method, it was possible to obtain an accurate separation between the two dispersive and polar free energies of adsorption of polar solvents on the two COF surfaces.

2. IGC Method and Materials

The chromatographic measurements obtained in other studies [18,19] led to the free energy of adsorption ΔG_a^0 or $RT \ln V_n$ of adsorbed molecules on solid substrates as a function of temperature. The proposed method is that using the deformation polarizability α_{0X} of the adsorbed molecule and the harmonic mean of the ionization energies, given by Relation (5):

$$\Delta G_a^0(T) = -\frac{\alpha_{0S}}{H^6} \left[\frac{3\mathcal{N}}{2(4\pi\varepsilon_0)^2} \left(\frac{\varepsilon_S \varepsilon_X}{(\varepsilon_S + \varepsilon_X)} \alpha_{0X} \right) \right] + \Delta G_a^{sp}(T) \quad (5)$$

where \mathcal{N} is Avogadro's number, ε_0 the permittivity of vacuum, S denotes the solid particle and X the solvent molecule separated by a distance H . By choosing $\mathcal{P}_{SX} = \frac{\varepsilon_S \varepsilon_X}{(\varepsilon_S + \varepsilon_X)} \alpha_{0X}$ as a thermodynamic parameter and considering the adsorption of n-alkanes on the solid material, Equation (6) can be then written as follows:

$$RT \ln V_n(\text{n-alkane}) = A \left[\frac{3\mathcal{N}}{2(4\pi\varepsilon_0)^2} \mathcal{P}_{SX(\text{n-alkane})} \right] - C \quad (6)$$

where C is an interaction constant of the adsorbed molecule and A is given by Equation (7):

$$A = \frac{\alpha_{0S}}{H^6} \quad (7)$$

The variations in $RT \ln Vn$ (n-alkane) as a function of $\frac{3N}{2(4\pi\epsilon_0)^2} \mathcal{P}_{SX(n-alkane)}$ gave a straight line called the “n-alkanes straight line”. In the case of polar molecule X, it was possible to deduce the specific or polar free energy of the interaction between the adsorbed molecule and the solid surface from Equation (8) at a temperature T:

$$-\Delta G_a^{sp}(T) = RT \ln Vn(X) - A \left[\frac{3N}{2(4\pi\epsilon_0)^2} \mathcal{P}_{SX} \right] + C \quad (8)$$

The determination of $(-\Delta G_a^{sp}(T))$ versus the temperature led to the specific enthalpy $-\Delta H_a^{sp}$ and entropy $-\Delta S_a^{sp}$ of polar solvents and therefore to the Lewis acid–base constants K_A and K_D by using Equation (9):

$$-\Delta H^{Sp} = K_A \times DN + K_D \times AN \quad (9)$$

where AN and DN are the electron donor and acceptor numbers of the polar molecule, respectively, calculated by Gutmann [43] and corrected by Riddle and Fowkes [44]. Several organic solvents were used in this study: n-alkanes including n-pentane, n-hexane, n-heptane and n-octane; polar probes including Lewis acid solvents such as dichloromethane, basic solvents such as ethyl acetate, diethyl ether and tetrahydrofuran and amphoteric solvents such as acetonitrile. The experimental conditions of the IGC technique were identical to those given in previously published papers [32–34].

3. Experimental Results

3.1. Polar Surface Interactions between Solid Materials and Organic Molecules

Table 1 gathers the different values of α_{0X} and \mathcal{P}_{SX} of the various organic solvents and their ionization energies obtained from the *Handbook of Physics and Chemistry* [45]. The values of the harmonic mean of ionization energies and parameter $\frac{3N}{2(4\pi\epsilon_0)^2} \mathcal{P}_{SX}$ are presented in Table 2. The values presented in Tables 1 and 2 allowed the determination of the values of the polar free surface energy $(-\Delta G_a^{sp}(T))$ of the polar solvents adsorbed on the single-crystalline and polycrystalline TAPPy-TPA-COFs as a function of the temperature T. The obtained results are presented in Table 3.

Table 1. Values of deformation polarizability and ionization energy of the various molecules.

Molecule	ϵ_X (eV)	α_0 (10^{-30} m^3)	α_0 ($10^{-40} \text{ C m}^2/\text{V}$)
n-pentane	10.28	9.99	11.12
n-hexane	10.13	11.90	13.24
n-heptane	9.93	13.61	15.14
n-octane	9.80	15.90	17.69
CH ₂ Cl ₂	11.32	7.21	8.02
Diethyl ether	9.51	9.47	10.54
Tetrahydrofuran	9.38	8.22	9.15
Ethyl acetate	10.01	9.16	10.19
Acetonitrile	12.20	4.44	4.94
TAPPy-TPA-COF	7.88	22.38	24.9

Table 2. Values of the harmonic means of the ionization energies $\frac{\epsilon_S \epsilon_X}{(\epsilon_S + \epsilon_X)}$ of TAPPy-TPA-COFs and organic solvents and the parameter $\frac{3N}{2(4\pi\epsilon_0)^2} \mathcal{P}_{S-X}$ for the various organic molecules.

Molecule	$\frac{\epsilon_S \epsilon_X}{(\epsilon_S + \epsilon_X)}$ (10^{-19} J)	$\frac{3N}{2(4\pi\epsilon_0)^2} \mathcal{P}_{S-X}$ (10^{-15} SI)
n-pentane	7.137	57.886
n-hexane	7.092	68.513
n-heptane	7.030	77.674
n-octane	6.989	90.213
CH ₂ Cl ₂	7.433	43.512
Diethyl ether	6.895	53.010
Tetrahydrofuran	6.852	45.726
Ethyl acetate	7.055	52.462
Acetonitrile	7.660	27.613

Table 3. Values of $(-\Delta G_a^{sp}(T))$ kJ/mol of polar molecules adsorbed on the single-crystalline and polycrystalline TAPPy-TPA-COFs.

Single-Crystalline (SC)				
T (K)	393.15	403.15	413.15	423.15
CH ₂ Cl ₂	2.161	2.036	1.719	1.691
Diethyl ether	1.343	1.229	0.966	1.043
THF	5.031	4.879	4.565	4.385
Ethyl Acetate	4.149	3.925	3.683	3.580
Acetonitrile	6.794	6.364	6.069	5.702
Polycrystalline (PC)				
T (K)	393.15	403.15	413.15	423.15
CH ₂ Cl ₂	3.317	3.019	3.382	2.998
Diethyl ether	2.245	2.049	1.805	2.024
THF	6.463	5.978	6.302	5.824
Ethyl Acetate	6.058	5.685	5.788	5.443
Acetonitrile	11.426	10.550	10.899	9.892

The values given in Table 3 showed that the polycrystalline (PC) COFs exhibited more acid–base interactions than single-crystalline (SC) COFs for all polar solvents with an increase in solvents with amphoteric character. Next, the polar surface energy of interaction $\gamma_{S-X}^p(T)$ reflecting the polarity of the adsorbate X was directly calculated from the values of $(-\Delta G_a^{sp}(T))$ given in Table 3 by using the values of the surface areas of polar molecules as a function of the temperature given by the Hamieh thermal model [32–34]. The obtained results for the two COFs are presented in Table 4.

Table 4. Values of polar surface energy of interaction $\gamma_{S-X}^p(T)$ (mJ/m²) of polar molecules adsorbed on the single-crystalline and polycrystalline TAPPy-TPA-COFs.

Single-Crystalline (SC)				
T (K)	393.15	403.15	413.15	423.15
CH ₂ Cl ₂	8.1	7.5	6.2	6.0
Diethyl ether	4.0	3.6	2.8	3.0
THF	21.0	20.3	18.9	18.1
Ethyl Acetate	13.8	13.0	12.1	11.7
Acetonitrile	20.7	19.2	18.1	16.8
Polycrystalline (PC)				
T (K)	393.15	403.15	413.15	423.15
CH ₂ Cl ₂	12.5	11.1	12.3	10.7
Diethyl ether	6.7	6.0	5.2	5.8
THF	27.0	24.9	26.1	24.0
Ethyl Acetate	20.2	18.8	19.0	17.7
Acetonitrile	34.7	31.8	32.5	29.2

Table 4 shows that the polar surface energy of interaction γ_{S-X}^p of polar molecules adsorbed on polycrystalline (PC) is about 1.5 times greater than that of single-crystalline (SC) COFs for the different molecules at any temperature. A decrease of γ_{S-X}^p of the various polar solvents was observed when the temperature increased. The values in Table 4 proved that the largest polar surface interaction was obtained with acetonitrile followed by tetrahydrofuran and ethyl acetate. This is certainly due to the presence of a π -electron-rich triple bond that could enhance π - π interactions between acetonitrile and the two COFs and free pairs of electrons in tetrahydrofuran and ethyl acetate molecules.

3.2. Lewis Acid and Base Surface Energies of COFs

The Van Oss relation was used to determine the Lewis acid γ_s^+ and base γ_s^- surface energies of the two COFs. Van Oss et al. proposed [46] the following equation:

$$-\Delta G_a^{sp}(T) = 2Na \left(\sqrt{\gamma_l^- \gamma_s^+} + \sqrt{\gamma_l^+ \gamma_s^-} \right) \quad (10)$$

where γ_l^+ and γ_l^- are the respective acid and base contributions of the Lewis base surface energy of the solvent adsorbed on COFs.

The two monopolar solvents used were ethyl acetate (EA) and dichloromethane (CH₂Cl₂) characterized by $\gamma_{EA}^+ = 0$, $\gamma_{EA}^- = 19.2$ mJ/m² and $\gamma_{CH_2Cl_2}^+ = 5.2$ mJ/m², $\gamma_{CH_2Cl_2}^- = 0$. This led to the determination of Lewis acid and base surface energies of the COFs by using Relation (11):

$$\begin{cases} \gamma_s^+ = \frac{[\Delta G_a^{sp}(T)(EA)]^2}{4N^2[a(EA)]^2 \gamma_{EA}^-} \\ \gamma_s^- = \frac{[\Delta G_a^{sp}(T)(CH_2Cl_2)]^2}{4N^2[a(CH_2Cl_2)]^2 \gamma_{CH_2Cl_2}^+} \end{cases} \quad (11)$$

The values of $\Delta G_a^{sp}(T)(EA)$ and $\Delta G_a^{sp}(T)(CH_2Cl_2)$ as a function of the temperature are given by Table 3, whereas the surface area $a(EA)$ and $a(CH_2Cl_2)$ are taken from reference [32]. Furthermore, the total acid–base surface energy γ_s^{AB} of the two COFs was obtained from Relation (12).

$$\gamma_s^{AB} = 2\sqrt{\gamma_s^+ \gamma_s^-} \quad (12)$$

Relations (11) and (12) allowed the determination the values of γ_s^+ , γ_s^- and γ_s^{AB} of single-crystalline and polycrystalline TAPPy-TPA-COFs. The obtained results are given in Table 5.

Table 5. Values of the polar acid and base surface energies γ_s^+ , γ_s^- and γ_s^{AB} (mJ/m²) of single-crystalline and polycrystalline TAPPy-TPA-COFs.

COF	Single-Crystalline (SC)			Polycrystalline (PC)		
	T (K)	γ_s^-	γ_s^+	γ_s^{AB}	γ_s^-	γ_s^+
393.15	2.54	2.07	4.59	7.46	4.42	11.48
403.15	2.21	1.82	4.01	6.37	3.81	9.85
413.15	1.55	1.57	3.11	5.33	3.50	8.63
423.15	1.46	1.45	2.92	4.38	3.19	7.47

Table 5 shows that the highest values of the polar acid and base surface energies were obtained for polycrystalline TAPPy-TPA-COF, whereas those of single-crystalline TAPPy-TPA-COF were very weak; this proves the non-polar character of this material. This result confirmed the previous results obtained regarding the specific free energy of adsorption on the two COFs and their polar surface energy of interaction $\gamma_{SX}^p(T)$. The results showed that the total acid–base surface energy γ_s^{AB} of a polycrystalline surface is about 2.3 times larger than that of a single-crystalline surface with more accentuated values of the basic surface energy γ_s^- in the case of polycrystalline COF. The values of γ_s^- and γ_s^+ for the single-crystalline surface are very close but much lower than those of the polycrystalline COF material. Furthermore, it was observed that a decrease in the contributions of different acid–base components of COFs occurs when the temperature increases.

The values of the dispersive component of the surface energy of the two COF materials given in Table 6 were determined as a function of the temperature by using the thermal model [32]. On the other hand, the values of γ_s^{AB} in Table 5 and Relation (13) allowed for the calculation of the total surface energy γ_s^{LW} , also called the Lifshitz–Van der Waals (LW) surface energy of single-crystalline and polycrystalline COFs. The results given in Table 6 show that the polycrystalline surface exhibited highest dispersive, polar and total surface energies at about 1.5 times greater than those of the single-crystalline COF material.

$$\gamma_s^{LW} = \gamma_s^d + \gamma_s^{AB} \quad (13)$$

Table 6. Values of the dispersive γ_s^d and total $\gamma_s^{tot.}$ surface energies (mJ/m²) of single-crystalline and polycrystalline COFs.

COF	Single-Crystalline (SC)		Polycrystalline (PC)	
	T (K)	γ_s^d	γ_s^{LW}	γ_s^d
393.15	66.23	70.82	93.80	105.28
403.15	56.47	60.48	78.18	88.03
413.15	47.47	50.59	69.38	78.01
423.15	38.84	41.75	52.03	59.50

3.3. Lewis Acid–Base Parameters

The values of $\Delta G_a^{sp}(T)$ of the various polar molecules given in Table 3 as a function of the temperature led to the determination of their polar or specific enthalpy $-\Delta H_a^{sp}$ and entropy $-\Delta S_a^{sp}$ of adsorption on the two COFs. Table 7 gives the obtained results. The previous results concerning the polarity of the two studied COFs were here confirmed by the values in Table 7 of the polar enthalpy of adsorption of the polar solvents. All calculated

values of $-\Delta H_a^{sp}$ of adsorption on the polycrystalline COF were found to be higher than those of the single-crystalline COF.

Table 7. Values of $-\Delta H_a^{sp}$ and $-\Delta S_a^{sp}$ of adsorption on the single-crystalline and polycrystalline COFs.

Single-Crystalline (SC)		
Polar Solvent	$-\Delta S_a^{sp}$ ($\text{JK}^{-1}\text{mol}^{-1}$)	$-\Delta H_a^{sp}$ (kJmol^{-1})
CH_2Cl_2	22.1	10.868
Diethyl ether	18.9	8.7816
THF	22.5	13.906
Ethyl acetate	19.5	11.792
Acetonitrile	35.7	20.819
Polycrystalline (PC)		
Polar Solvent	$-\Delta S_a^{sp}$ ($\text{JK}^{-1}\text{mol}^{-1}$)	$-\Delta H_a^{sp}$ (kJmol^{-1})
CH_2Cl_2	21.4	11.756
Diethyl ether	22	10.899
THF	35.6	20.404
Ethyl acetate	24.5	15.652
Acetonitrile	59.6	34.712

In order to better understand the Lewis acid–base behavior of the two COF surfaces, the acid–base parameters were determined by using Equation (9) and the results given in Table 7. The variations in $\left(\frac{-\Delta H_a^{sp}}{AN'}\right)$ as a function of $\left(\frac{DN'}{AN'}\right)$ of polar molecules adsorbed on the two COFs are plotted in Figure 2. The obtained straight line exhibits two different slopes showing a net difference between the Lewis acid–base constants of the studied materials and especially a larger acidic constant for the polycrystalline surface. The obtained results are given in Table 8.

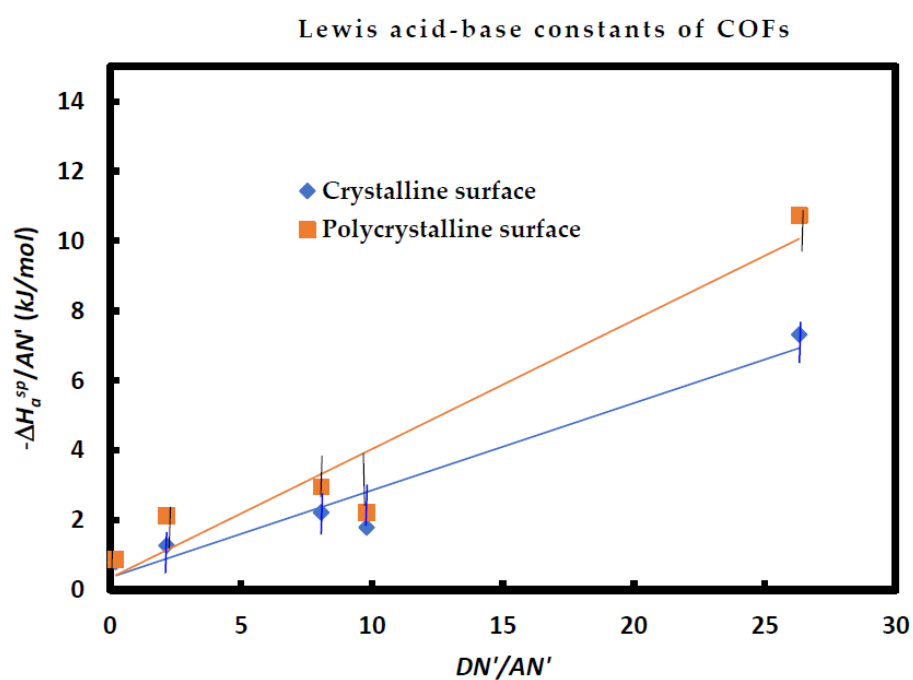


Figure 2. Variations in $\left(\frac{-\Delta H_a^{sp}}{AN'}\right)$ as a function of $\left(\frac{DN'}{AN'}\right)$ of polar molecules adsorbed on crystalline and polycrystalline surfaces.

Table 8. Values of the enthalpic acid–base constants K_A and K_D and the entropic acid–base constants ω_A and ω_D of the single-crystalline and polycrystalline COFs with their corresponding acid–base ratios and linear regression coefficients.

COF Surfaces	K_A	K_D	K_D/K_A	R^2	$10^3 \cdot \omega_A$	$10^3 \cdot \omega_D$	ω_D/ω_A	R^2
Single-crystalline COF	0.149	0.213	1.430	0.947	0.236	0.570	2.413	0.9724
Polycrystalline COF	0.221	0.205	0.930	0.924	0.386	0.358	0.928	0.9361

Table 8 clearly shows the Lewis amphoteric character of the single and polycrystalline COFs with a higher Lewis basicity for the single-crystalline (SC) surface and higher Lewis acidity for the polycrystalline (PC) surface. It was also observed that $\frac{K_A(\text{Polycrystalline COF})}{K_A(\text{Single-crystalline COF})} = 1.48$ and $\frac{K_D(\text{Polycrystalline COF})}{K_D(\text{Single-crystalline COF})} = 0.96$, showing that the polycrystalline COF surface was more acidic than the single-crystalline COF surface, whereas their basicity was comparable. The same results were confirmed by the Lewis entropic acid–base parameters. The obtained results of the Lewis acid–base constants of the two COFs once again confirmed those obtained for the polar enthalpy and acid–base surface energies of the SC and PC surfaces.

The various results presented in Tables 3, 5, 7 and 8 clearly show that the polar surface interactions between the different polar solvents (dichloromethane, diethyl ether, THF, ethyl acetate and acetonitrile) and the polycrystalline COF are higher than those of the single-crystalline COF. It was shown in Table 3 that the free polar energies $-\Delta G_a^{sp}$ of the different polar molecules adsorbed on the PC surface are at least 1.5 times higher than those of the same probes adsorbed on SC surface at different temperatures, and the difference increases when the temperature increases. The results in Table 4 also show the same observation on the highest polar surface energy of interaction γ_{S-X}^p of polycrystalline COF. This difference in the polar parameters of the two materials was confirmed by the results in Table 8 showing an acidity of the PC COF that is 1.5 times higher than that of the SC material.

3.4. Consequences and Discussion of the New Results on COF Surfaces

3.4.1. London Dispersive and Polar Energies of Interaction

The new proposed parameter $\mathcal{P}_{SX} = \frac{\epsilon_S \epsilon_X}{(\epsilon_S + \epsilon_X)} \alpha_{0X}$ led to a net separation between the London dispersion energy and the polar free energy of the adsorption of polar organic molecules and COF surfaces. The new method quantified the London dispersive energy of the interaction between the two COFs and adsorbed n-alkanes by using Relation (14) that also led to the determination of London dispersive and polar free energies of all solvents. The results of London dispersion interactions were presented in Table 9.

$$\Delta G_a^d(T) = A \left[\frac{3\mathcal{N}}{2(4\pi\epsilon_0)^2} \mathcal{P}_{SX} \right] \quad (14)$$

Table 9 also shows the higher values of the London dispersion interactions of the polycrystalline COF than those obtained for the single-crystalline COF for all used organic molecules and all temperatures. The results given in Table 9 allowed for the determination of the London dispersive enthalpy and entropy of interaction for the two COFs. The obtained values are given in Table 10.

Table 9. Values of London dispersion interactions $-\Delta G_a^d(T)$ (kJmol⁻¹) of organic molecules adsorbed on single-crystalline and polycrystalline COFs.

Single-Crystalline COF				
T (K)	393.15	403.15	413.15	423.15
n-pentane	19.861	19.073	18.431	17.962
n-hexane	23.507	22.575	21.815	21.260
n-heptane	26.650	25.593	24.731	24.102
n-octane	30.952	29.725	28.724	27.993
CH ₂ Cl ₂	14.929	14.337	13.854	13.502
Diethyl ether	18.188	17.467	16.878	16.449
Tetrahydrofuran	15.689	15.067	14.559	14.189
Ethyl acetate	18.000	17.286	16.704	16.279
Acetonitrile	9.474	9.098	8.792	8.568
Polycrystalline COF				
T (K)	393.15	403.15	413.15	423.15
n-pentane	23.664	22.471	22.298	20.793
n-hexane	28.008	26.597	26.391	24.610
n-heptane	31.753	30.153	29.920	27.900
n-octane	36.879	35.021	34.750	32.405
CH ₂ Cl ₂	17.788	16.891	16.761	15.630
Diethyl ether	21.671	20.579	20.420	19.041
Tetrahydrofuran	18.693	17.751	17.614	16.425
Ethyl acetate	21.447	20.366	20.209	18.845
Acetonitrile	11.288	10.719	10.636	9.918

Table 10. Values of London dispersion entropy $-\Delta S_a^d$ and enthalpy $-\Delta H_a^d$ of organic molecules adsorbed on single-crystalline and polycrystalline COF surfaces.

COF Surfaces	Single-Crystalline (SC)		Polycrystalline (PC)	
	$-\Delta S_a^d$ (JK ⁻¹ mol ⁻¹)	$-\Delta H_a^d$ (kJmol ⁻¹)	$-\Delta S_a^d$ (JK ⁻¹ mol ⁻¹)	$-\Delta H_a^d$ (kJmol ⁻¹)
n-pentane	63.4	44.702	87.9	58.171
n-hexane	75	52.909	104	68.85
n-heptane	85.1	59.983	117.9	78.056
n-octane	98.8	69.667	136.9	90.657
CH ₂ Cl ₂	47.6	33.602	66.1	43.726
Diethyl ether	58	40.937	80.5	53.271
Tetrahydrofuran	50.1	35.312	69.4	45.951
Ethyl acetate	57.4	40.514	79.6	52.721
Acetonitrile	30.2	21.324	41.9	27.749

It was observed that the obtained values of the dispersive and polar parameters of the polycrystalline surface are higher than those obtained for the single-crystalline surface. The results given in Table 10 are visualized in Figure 3 through the variations in London dispersion enthalpy $-\Delta H_a^d$ as a function of London dispersion entropy $-\Delta S_a^d$ for the two COFs as well as the variations corresponding to polar or specific variables of adsorption. A perfect linearity (with $R^2 = 1$) was observed. The obtained straight lines are given

below. Equation (15) was obtained in the case of single-crystalline (SC) COFs, whereas Equation (16) was given for polycrystalline (PC) COFs.

$$\Delta H_a^d \left(\text{kJmol}^{-1} \right) (\text{SC}) = 0.7046 \Delta S_a^d \left(\text{JK}^{-1}\text{mol}^{-1} \right) (\text{SC}) - 0.0501 \quad (15)$$

$$\Delta H_a^d \left(\text{kJmol}^{-1} \right) (\text{PC}) = 0.6622 \Delta S_a^d \left(\text{JK}^{-1}\text{mol}^{-1} \right) (\text{PC}) + 0.0201 \quad (16)$$

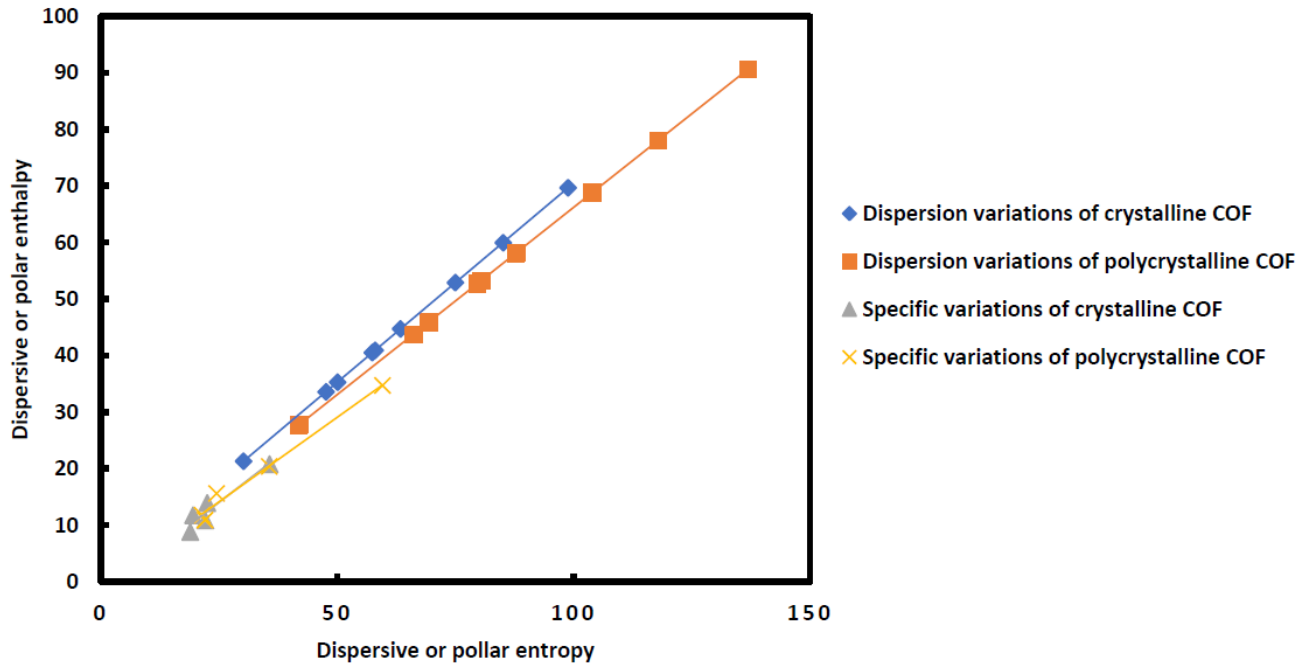


Figure 3. Variations in London dispersion enthalpy $-\Delta H_a^d$ (kJmol^{-1}) as a function of London dispersion entropy $-\Delta S_a^d$ ($\text{JK}^{-1}\text{mol}^{-1}$) for the two COFs and the variations corresponding to the polar or specific variables $-\Delta H_a^{sp}$ (kJmol^{-1}) and $-\Delta S_a^{sp}$ ($\text{JK}^{-1}\text{mol}^{-1}$) of adsorption.

The evolution of the specific enthalpy as a function of the specific entropy of the two COF surfaces was also plotted in Figure 2 and led to Equations (17) and (18).

$$\Delta H_a^{sp} \left(\text{kJmol}^{-1} \right) (\text{SC}) = 0.6436 \Delta S_a^{sp} \left(\text{JK}^{-1}\text{mol}^{-1} \right) (\text{SC}) + 2.0455 \quad (17)$$

$$\Delta H_a^{sp} \left(\text{kJmol}^{-1} \right) (\text{PC}) = 0.5978 \Delta S_a^{sp} \left(\text{JK}^{-1}\text{mol}^{-1} \right) (\text{PC}) + 0.8168 \quad (18)$$

These results motivated us to propose in both cases of dispersion and polar enthalpies and entropies the general Equations (19) and (20) relative to the respective dispersion and polar cases:

$$\Delta H_a^d (X) = T_S^d \Delta S_a^d (X) + \Delta G_a^d (S) \quad (19)$$

$$\Delta H_a^{sp} (X) = T_S^{sp} \Delta S_a^{sp} (X) + \Delta G_a^{sp} (S) \quad (20)$$

where T_S^d and $-\Delta G_a^d(S)$ are two new characteristics of solid substrates representing a dispersion temperature and free dispersion energy of the solid, respectively, and T_S^{sp} and $-\Delta G_a^{sp}(S)$ represent those corresponding to the polar interaction of the solid. It was deduced that every solid surface was characterized by two dispersion parameters T_S^d and $-\Delta G_a^d(S)$ and two polar parameters T_S^{sp} and $-\Delta G_a^{sp}(S)$. By combining the two dispersion and polar effects, the following Relations (21) and (22) were obtained:

$$\Delta H_a^{d,sp} \left(\text{kJmol}^{-1} \right) (\text{SC}) = 0.7553 \Delta S_a^{d,sp} \left(\text{JK}^{-1}\text{mol}^{-1} \right) (\text{SC}) + 3.6943 \quad (21)$$

$$\Delta H_a^{d,sp} \left(\text{kJmol}^{-1} \right) (PC) = 0.6879 \Delta S_a^{d,sp} \left(\text{JK}^{-1}\text{mol}^{-1} \right) (PC) + 2.7881 \quad (22)$$

Table 10 and Figure 3 led to the results in Table 11 showing the various characteristics of the two COFs.

Table 11. Values of the new characteristics of single-crystalline and polycrystalline TAPPy-TPA-COF surfaces. These values were directly deduced from Relations (15) to (22).

COF Surfaces	Single-Crystalline (SC)	Polycrystalline (PC)
T_S^d (K)	704.6	662.2
T_S^{sp} (K)	643.6	597.8
$-\Delta G_a^d(S)$ (J/mol)	−50.1	20.1
$-\Delta G_a^{sp}(S)$ (J/mol)	2046	817
T_S (K)	755.3	687.9
$-\Delta G_a(S)$ (J/mol)	3694	2788

These new findings deserve more reflection and deeper investigation. The dispersion temperature was shown to be higher than the polar temperature for the two COFs. However, the dispersion and polar temperatures of the single-crystalline COF were higher than those of the polycrystalline COF. The values of the intrinsic temperature T_S and free energy $-\Delta G_a(S)$ of the two materials are given in Table 11. It was observed that the highest intrinsic temperature was obtained for the single-crystalline COF ($T_S(SC) = 755.3$ K) with a difference compared to that of polycrystalline COF equal to 67.4 K. These values were probably related to the melting point or decomposition temperature of these materials.

3.4.2. Comparison with the Values Obtained by Using the Donnet et al. Method

In order to compare the results of this work with those obtained when using the Donnet et al. method [27], the values of specific free energies of polar solvents adsorbed on single-crystalline and polycrystalline surfaces are shown in Table 12.

The comparison between the results of this work and those obtained by using the Donnet et al. method [27] (Tables 3 and 12) showed very large difference due to the insufficiency of the approach proposed by Donnet et al. [27] that neglected the role of the harmonic mean of the ionization energies of organic molecules and solid surface. The results of Table 12 clearly show an important difference between the values obtained by the two methods. Indeed, the ratio $\frac{\Delta G_a^{sp}(\text{Donnet et al.})}{\Delta G_a^{sp}(\text{Hamieh})}$ reaches two for some polar molecules such as diethyl ether (Table 13). Furthermore, a negative value of the specific free energy of dichloromethane was obtained by the Donnet et al. method. This negative value of $(-\Delta G_a^{sp}(T))$ cannot be acceptable for a polar molecule. This resulted from the large approximation used by Donnet et al. that neglected the role of the harmonic mean of the ionization energies. The same observations were shown for the ratios $\frac{\Delta S_a^{sp}(\text{Donnet et al.})}{\Delta S_a^{sp}(\text{Hamieh})}$ and $\frac{\Delta H_a^{sp}(\text{Donnet et al.})}{\Delta H_a^{sp}(\text{Hamieh})}$ that varied from 0.6 to 0.8 with also negative values when using the Donnet method (Table 13). The results presented in Table 13 clearly show the large deviation between the values of the different thermodynamic parameters obtained by the Donnet et al. method and those obtained by this work. Furthermore, negative values were also obtained for the Lewis basic constants of Donnet et al. method [27] showing the non-validity of their approach in this case.

Table 12. Values of $-\Delta G_a^{sp}(T)$ (kJ/mol), $-\Delta S_a^{sp}$ and ΔH_a^{sp} of polar molecules adsorbed on single-crystalline and polycrystalline COFs by using the Donnet et al. method [27].

Single-Crystalline Surface						
T (K)	393.15	403.15	413.15	423.15	$-\Delta S_a^{sp}$ (JK ⁻¹ mol ⁻¹)	$-\Delta H_a^{sp}$ (kJmol ⁻¹)
CH ₂ Cl ₂	-6.994	-6.753	-6.774	-6.586	-12	-11.684
Diethyl ether	2.422	2.268	1.970	2.023	14.9	8.2649
THF	5.271	5.114	4.791	4.607	23.1	14.385
Ethyl Acetate	3.047	2.871	2.663	2.587	15.9	9.2637
Acetonitrile	7.794	7.329	7.001	6.613	38.7	22.982
Polycrystalline Surface						
T (K)	393.15	403.15	413.15	423.15	$-\Delta S_a^{sp}$ (JK ⁻¹ mol ⁻¹)	$-\Delta H_a^{sp}$ (kJmol ⁻¹)
CH ₂ Cl ₂	-7.589	-7.334	-6.894	-6.584	-34.6	-21.202
Diethyl ether	3.527	3.272	3.016	3.154	13.7	8.8457
THF	6.744	6.251	6.571	6.076	16.9	13.286
Ethyl Acetate	4.743	4.441	4.551	4.291	12.5	9.5951
Acetonitrile	12.608	11.680	12.019	10.938	46.7	30.864

Table 13. Values of the ratios $\frac{\Delta G_a^{sp}(\text{Donnetetal.})}{\Delta G_a^{sp}(\text{Hamieh})}$, $\frac{\Delta S_a^{sp}(\text{Donnetetal.})}{\Delta S_a^{sp}(\text{Hamieh})}$ and $\frac{\Delta H_a^{sp}(\text{Donnetetal.})}{\Delta H_a^{sp}(\text{Hamieh})}$ of polar molecules adsorbed on single-crystalline and polycrystalline COFs by using the Donnet et al. method [27].

Single-Crystalline Surface						
T (K)	393.15	403.15	413.15	423.15	$-\Delta S_a^{sp}$ (JK ⁻¹ mol ⁻¹)	$-\Delta H_a^{sp}$ (kJmol ⁻¹)
CH ₂ Cl ₂	-3.24	-3.32	-3.94	-3.89	-0.54	-1.08
Diethyl ether	1.80	1.85	2.04	1.94	0.79	0.94
THF	1.05	1.05	1.05	1.05	1.03	1.03
Ethyl Acetate	0.73	0.73	0.72	0.72	0.82	0.79
Acetonitrile	1.15	1.15	1.15	1.16	1.08	1.10
Polycrystalline Surface						
T (K)	393.15	403.15	413.15	423.15	$-\Delta S_a^{sp}$ (JK ⁻¹ mol ⁻¹)	$-\Delta H_a^{sp}$ (kJmol ⁻¹)
CH ₂ Cl ₂	-2.29	-2.43	-2.04	-2.20	-1.62	-1.80
Diethyl ether	1.57	1.60	1.67	1.56	0.62	0.81
THF	1.04	1.05	1.04	1.04	0.47	0.65
Ethyl Acetate	0.78	0.78	0.79	0.79	0.51	0.61
Acetonitrile	1.10	1.11	1.10	1.11	0.78	0.89

3.4.3. Approximative Evaluation of the Separation Distance H between Particles

By using the new method, it was possible to determine the average separation distance H between the solid particle and the organic molecule as a function of the temperature. The results given in Table 14 led to the average separation distance H that weakly varied as a function of the temperature. The distance H was approximately the same for the two COF materials (H was between 6.2 and 6.4 Å).

Table 14. Values of the average separation distance H (Å) between the two solid substrates and the organic molecules at different temperatures.

T (K)	393.15	403.15	413.15	423.15
Single-Crystalline Surface	6.34	6.39	6.42	6.45
Polycrystalline Surface	6.16	6.20	6.22	6.30

Furthermore, the total potential energy of interaction $I_{Tot.}(r)$ between a solid particle and an organic molecule, separated by a distance r , is equal to the sum of the repulsive $I_{Rep.}(r)$ energy and Van der Waals attractive $I_{VDW}(r)$ energy with their respective interaction constants $A_{Rep.}$ and A_{VDW} .

$$I_{Tot.}(r) = I_{Rep.}(r) + I_{VDW}(r) \quad (23)$$

The expressions of $I_{Rep.}(r)$ and $I_{VDW}(r)$ are respectively given by the following:

$$\begin{aligned} I_{Rep.}(r) &= \frac{A_{Rep.}}{r^{12}} \\ I_{VDW}(r) &= -\frac{A_{VDW}}{r^6} \end{aligned} \quad (24)$$

And $I_{Tot.}(r)$ is then written by the well-known Lennard-Jones equation:

$$I_{Tot.}(r) = \frac{A_{Rep.}}{r^{12}} - \frac{A_{VDW}}{r^6} \quad (25)$$

The total potential energy of interaction $I_{Tot.}(r)$ is cancelled for r_0 equal to the following:

$$r_0 = \left(\frac{A_{Rep.}}{A_{VDW}} \right)^{1/6} \quad (26)$$

whereas $I_{Tot.}(r)$ reaches its minimum energy for a minimal distance H given by the following:

$$H = r_{min.} = \left(2 \frac{A_{Rep.}}{A_{VDW}} \right)^{1/6} \quad (27)$$

The relation between r_0 and H is then given by Equation (28):

$$r_0 = \frac{H}{2^{1/6}} \approx 0.891H \quad (28)$$

This led to the results given in Table 15.

Table 15. Values of r_0 (Å) and the ratio $A_{Rep.}/A_{VDW}$ (Å⁶) at different temperatures.

TAPPy-TPA-COFS	Single-Crystalline Surface		Polycrystalline Surface	
	T(K)	r_0	$A_{Rep.}/A_{VDW}$	r_0
393.15	5.65	1.335	5.49	1.328
403.15	5.69	1.336	5.54	1.330
413.15	5.72	1.337	5.54	1.330
423.15	5.75	1.338	5.61	1.333
Average values	5.70	1.34	5.55	1.33

Table 14 shows a slight variation in both r_0 and the ratio $A_{Rep.}/A_{VDW}$ when the temperature varies. A weak decrease in these parameters in the case of the two COF surfaces was noticed. It can be concluded from Table 14 that there is no significant effect of

the crystallinity of COFs on the distance r_0 (which cancelled the total energy of interaction of the solid surface) nor any appreciable effect on the ratio of the two repulsive and attractive constants of interaction. This also led to identical values of the minimum potential energies of interaction of the two COFs. To further clarify the results presented in Table 14, the variations in the total energies of interaction of the two COFs are plotted in Figure 4 as a function of the separation distance H at 150 °C by using Equation (25) and the values given in Table 14. A small difference between the total energies of interaction of the two COFs was observed.

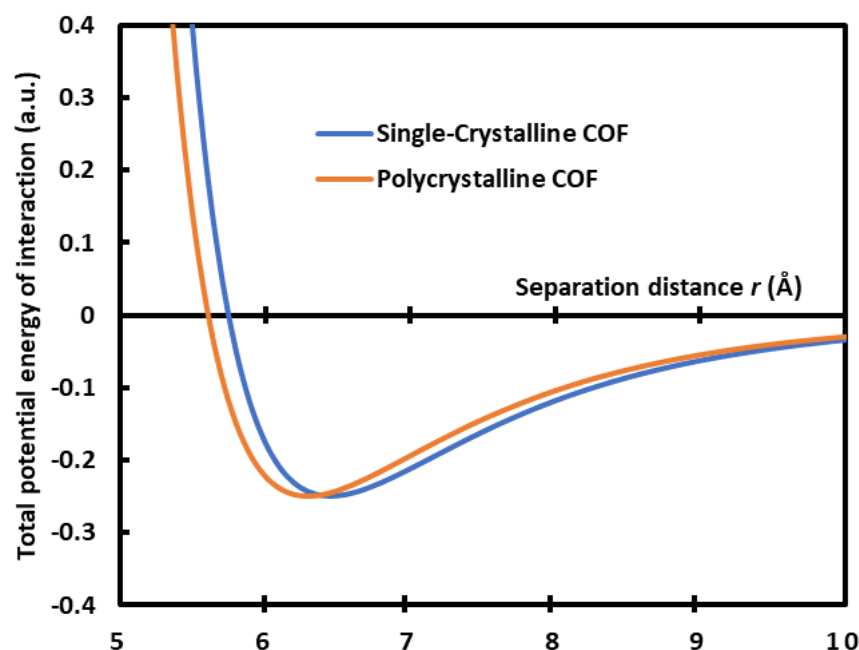


Figure 4. Variations in the total potential energy of interaction of the single-crystalline and polycrystalline COFs as a function of the separation distance r .

4. Conclusions

The London dispersive and polar surface thermodynamic parameters of single-crystalline and polycrystalline TAPPy-TPA-COFs were determined by the inverse gas chromatography technique (IGC) at infinite dilution. A new method for the separation of London dispersive and polar surface energies was proposed. A new intrinsic thermodynamic parameter $\mathcal{P}_{SX} = \frac{\varepsilon_S \varepsilon_X}{(\varepsilon_S + \varepsilon_X)} \alpha_{0X}$ was proposed which associates the deformation polarizability of molecules to the harmonic mean of the ionization energies of solid surface and organic molecules. The measurements of the net retention volume of the adsorbed solvents on COF surfaces and the use of the new parameter \mathcal{P}_{SX} as a function of the temperature led to the polar interaction energy $\Delta G_a^{sp}(T)$ of the different polar molecules adsorbed on the COF surfaces. This led to the different components of acid–base surface energies of solid surfaces and their total surface energy that all depend on the temperature. The new results showed that the values of the total acid–base surface energies of polycrystalline COFs ranged between 11.50 and 7.50 mJ/m² with a total surface energy equal to 105.3 mJ/m² at 120 °C; in contrast, the acid–base surface energies corresponding to the single-crystalline COFs were lower than 4.6 mJ/m² with a total surface energy equal to 70.8 mJ/m² at the same temperature.

All polar surface parameters of the polycrystalline COF surface revealed higher values than those obtained with the single-crystalline surface. An excellent linearity of $\left(\frac{-\Delta H_a^{sp}}{AN'}\right)$ versus $\left(\frac{DN'}{AN'}\right)$ of polar molecules adsorbed on the two COF surfaces was obtained and allowed an accurate determination of Lewis acid–base constants. The acidity of the polycrystalline surface was proved to be 1.5 times higher than that of the single-crystalline surface.

This new method allowed for the determination of the dispersive and specific enthalpy and entropy of adsorption, in both cases of single-crystalline (SC) and polycrystalline (PC), and proved the following equation:

$$\Delta H_a^{d,sp}(X) = T_S \Delta S_a^{d,sp}(X) + \Delta G_a^{d,sp}(S)$$

Two new characteristics of solid substrate T_S and $\Delta G_a^{d,sp}(S)$ were proposed representing the interaction temperature and the free interaction energy of the solid, respectively. The values of temperatures $T_S(SC) = 755.3$ K and $T_S(PC) = 687.9$ K showed that the highest intrinsic temperature was obtained by the single-crystalline COF with a difference between the two temperatures equal to 67.4 K. These values are probably related to the melting point or decomposition temperature of materials. This result has to be confirmed with other solid surfaces in future studies.

The comparison between the results of this work and those obtained by the Donnet et al. method showed very large differences in the values of the specific or polar surface interactions. This deviation resulted from the fact that the Donnet method neglected the effect of the harmonic mean of the ionization energies on the different surface thermodynamic parameters.

These new results also allowed the determination of an average value of the separation distance between the COF surfaces and the organic molecules equal to 5.70 Å for the crystalline COF and 5.55 Å for the polycrystalline form. This promising method will be used in other future studies for more accurate determination of the polar surface energy and Lewis acid–base surface energies of solid surfaces such as oxides, polymers, fibers, etc.

Funding: This research did not receive any specific grants or funds.

Data Availability Statement: There is no additional data. The original contributions presented in the study are included in the article.

Conflicts of Interest: The author declares no conflicts of interest.

References

1. Côté, A.P.; Benin, A.I.; Ockwig, N.W.; O’Keeffe, M.; Matzger, A.J.; Yaghi, O.M. Porous, Crystalline, Covalent Organic Frameworks. *Science* **2005**, *310*, 1166–1170. [[CrossRef](#)]
2. Shi, Y.; Yang, J.; Gao, F.; Zhang, Q. Covalent Organic Frameworks: Recent Progress in Biomedical Applications. *ACS Nano* **2023**, *17*, 1879–1905. [[CrossRef](#)]
3. Ding, S.-Y.; Gao, J.; Wang, Q.; Zhang, Y.; Song, W.-G.; Su, C.-Y.; Wang, W. Construction of Covalent Organic Framework for Catalysis: Pd/COF-LZU1 in Suzuki-Miyaura Coupling Reaction. *J. Am. Chem. Soc.* **2011**, *133*, 19816–19822. [[CrossRef](#)]
4. Sharma, R.K.; Yadav, P.; Yadav, M.; Gupta, R.; Rana, P.; Srivastava, A.; Zbořil, R.; Varma, R.S.; Antonietti, M.; Gawande, M.B. Recent development of covalent organic frameworks (COFs): Synthesis and catalytic (organic-electro-photo) applications. *Mater. Horiz.* **2020**, *7*, 411–454. [[CrossRef](#)]
5. Wang, X.; Han, X.; Zhang, J.; Wu, X.; Liu, Y.; Cui, Y. Homochiral 2D Porous Covalent Organic Frameworks for Heterogeneous Asymmetric Catalysis. *J. Am. Chem. Soc.* **2016**, *138*, 12332–12335. [[CrossRef](#)]
6. Fortea-Pérez, F.R.; Mon, M.; Ferrando-Soria, J.; Boronat, M.; Leyva-Pérez, A.; Corma, A.; Herrera, J.M.; Osadchii, D.; Gascon, J.; Armentano, D.; et al. The MOF-driven synthesis of supported palladium clusters with catalytic activity for carbene-mediated chemistry. *Nat. Mater.* **2017**, *16*, 760–766. [[CrossRef](#)]
7. Tu, W.; Xu, Y.; Yin, S.; Xu, R. Rational Design of Catalytic Centers in Crystalline Frameworks. *Adv. Mater.* **2018**, *30*, 1707582. [[CrossRef](#)]
8. Sun, T.; Xie, J.; Guo, W.; Li, D.-S.; Zhang, Q. Covalent-Organic Frameworks: Advanced Organic Electrode Materials for Rechargeable Batteries. *Adv. Energy Mater.* **2020**, *10*, 1904199. [[CrossRef](#)]
9. Tong, Y.; Sun, Z.; Wang, J.; Huang, W.; Zhang, Q. Covalent organic framework containing dual redox centers as an efficient anode in Li-ion batteries. *SmartMat* **2022**, *3*, 685–694. [[CrossRef](#)]
10. Zhong, L.; Fang, Z.; Shu, C.; Mo, C.; Chen, X.; Yu, D. Redox Donor-Acceptor Conjugated Microporous Polymers as Ultralong-Lived Organic Anodes for Rechargeable Air Batteries. *Angew. Chem. Int. Ed.* **2021**, *60*, 10164–10171. [[CrossRef](#)]
11. Wang, Z.; Zhang, S.; Chen, Y.; Zhang, Z.; Ma, S. Covalent organic frameworks for separation applications. *Chem. Soc. Rev.* **2020**, *49*, 708–735. [[CrossRef](#)]
12. Xu, S.; Zhang, Q. Recent progress in covalent organic frameworks as light-emitting materials. *Mater. Today Energy* **2021**, *20*, 100635. [[CrossRef](#)]

13. Guo, B.; Huang, Z.; Shi, Q.; Middha, E.; Xu, S.; Li, L.; Wu, M.; Jiang, J.; Hu, Q.; Fu, Z.; et al. Organic Small Molecule Based Photothermal Agents with Molecular Rotors for Malignant Breast Cancer Therapy. *Adv. Funct. Mater.* **2020**, *30*, 1907093. [CrossRef]
14. Zhao, F.; Liu, H.; Mathe, S.D.R.; Dong, A.; Zhang, J. Covalent Organic Frameworks: From Materials Design to Biomedical Application. *Nanomaterials* **2018**, *8*, 15. [CrossRef] [PubMed]
15. Giri, A.; Hopkins, P.E. Heat Transfer Mechanisms and Tunable Thermal Conductivity Anisotropy in Two-Dimensional Covalent Organic Frameworks with Adsorbed Gases. *Nano Lett.* **2021**, *21*, 6188–6193. [CrossRef] [PubMed]
16. Guo, J.; Jiang, D. Covalent Organic Frameworks for Heterogeneous Catalysis: Principle, Current Status, and Challenges. *ACS Cent. Sci.* **2020**, *6*, 869–879. [CrossRef]
17. Fu, X.; Lu, Z.; Yang, H.; Yin, X.; Xiao, L.; Hou, L. Imine-based covalent organic framework as photocatalyst for visible-light-induced atom transfer radical polymerization. *J. Polym. Sci.* **2021**, *59*, 2036–2044. [CrossRef]
18. Natraj, A.; Ji, W.; Xin, J.; Castano, I.; Burke, D.W.; Evans, A.M.; Strauss, M.J.; Ateia, M.; Hamachi, L.S.; Gianneschi, N.C.; et al. Single-Crystalline Imine-Linked Two-Dimensional Covalent Organic Frameworks Separate Benzene and Cyclohexane Efficiently. *J. Am. Chem. Soc.* **2022**, *144*, 19813–19824. [CrossRef]
19. Yusuf, K.; Natraj, A.; Li, K.; Ateia, M.; Al Othman, Z.A.; Dichtel, W.R. Inverse Gas Chromatography Demonstrates the Crystallinity-Dependent Physicochemical Properties of Two-Dimensional Covalent Organic Framework Stationary Phases. *Chem. Mater.* **2023**, *35*, 1691–1701. [CrossRef]
20. Vardhan, H.; Rummer, G.; Deng, A.; Ma, S. Large-Scale Synthesis of Covalent Organic Frameworks: Challenges and Opportunities. *Membranes* **2023**, *13*, 696. [CrossRef] [PubMed]
21. Matsumoto, M.; Dasari, R.R.; Ji, W.; Feriante, C.H.; Parker, T.C.; Marder, S.R.; Dichtel, W.R. Rapid, low temperature formation of imine-linked covalent organic frameworks catalyzed by metal triflates. *J. Am. Chem. Soc.* **2017**, *139*, 4999–5002. [CrossRef] [PubMed]
22. De la Peña Ruigómez, A.; Rodríguez-San-Miguel, D.; Stylianou, K.C.; Cavallini, M.; Gentili, D.; Liscio, F.; Milita, S.; Roscioni, O.M.; Ruiz-González, M.L.; Carbonell, C.; et al. Direct on-surface patterning of a crystalline laminar covalent organic framework synthesized at room temperature. *Chem. A Eur. J.* **2015**, *21*, 10666–10670. [CrossRef] [PubMed]
23. Saint-Flour, C.; Papirer, E. Gas-solid chromatography. A method of measuring surface free energy characteristics of short carbon fibers. 1. Through adsorption isotherms. *Ind. Eng. Chem. Prod. Res. Dev.* **1982**, *21*, 337–341. [CrossRef]
24. Saint-Flour, C.; Papirer, E. Gas-solid chromatography: Method of measuring surface free energy characteristics of short fibers. 2. Through retention volumes measured near zero surface coverage. *Ind. Eng. Chem. Prod. Res. Dev.* **1982**, *21*, 666–669. [CrossRef]
25. Saint-Flour, C.; Papirer, E. Gas-solid chromatography: A quick method of estimating surface free energy variations induced by the treatment of short glass fibers. *J. Colloid Interface Sci.* **1983**, *91*, 69–75. [CrossRef]
26. Schultz, J.; Lavielle, L.; Martin, C. The role of the interface in carbon fibre-epoxy composites. *J. Adhes.* **1987**, *23*, 45–60. [CrossRef]
27. Donnet, J.-B.; Park, S.; Balard, H. Evaluation of specific interactions of solid surfaces by inverse gas chromatography. *Chromatographia* **1991**, *31*, 434–440. [CrossRef]
28. Brendlé, E.; Papirer, E. A new topological index for molecular probes used in inverse gas chromatography for the surface nanorugosity evaluation, 2. Application for the Evaluation of the Solid Surface Specific Interaction Potential. *J. Colloid Interface Sci.* **1997**, *194*, 217–2224. [CrossRef] [PubMed]
29. Brendlé, E.; Papirer, E. A new topological index for molecular probes used in inverse gas chromatography for the surface nanorugosity evaluation, 1. Method of Evaluation. *J. Colloid Interface Sci.* **1997**, *194*, 207–216. [CrossRef] [PubMed]
30. Sawyer, D.T.; Brookman, D.J. Thermodynamically based gas chromatographic retention index for organic molecules using salt-modified aluminas and porous silica beads. *Anal. Chem.* **1968**, *40*, 1847–1850. [CrossRef]
31. Chehimi, M.M.; Pigois-Landureau, E. Determination of acid–base properties of solid materials by inverse gas chromatography at infinite dilution. A novel empirical method based on the dispersive contribution to the heat of vaporization of probes. *J. Mater. Chem.* **1994**, *4*, 741–745. [CrossRef]
32. Hamieh, T. Study of the temperature effect on the surface area of model organic molecules, the dispersive surface energy and the surface properties of solids by inverse gas chromatography. *J. Chromatogr. A* **2020**, *1627*, 461372. [CrossRef]
33. Hamieh, T. New methodology to study the dispersive component of the surface energy and acid–base properties of silica particles by inverse gas chromatography at infinite dilution. *J. Chromatogr. Sci.* **2022**, *60*, 126–142. [CrossRef] [PubMed]
34. Hamieh, T. New Physicochemical Methodology for the Determination of the Surface Thermodynamic Properties of Solid Particles. *AppliedChem* **2023**, *3*, 229–255. [CrossRef]
35. Hamieh, T.; Schultz, J. New approach to characterize physicochemical properties of solid substrates by inverse gas chromatography at infinite dilution. Some new methods to determine the surface areas of some molecules adsorbed on solid surfaces. *J. Chromatogr. A* **2002**, *969*, 17–47. [CrossRef]
36. Hamieh, T.; Schultz, J. Study of the adsorption of n-alkanes on polyethylene surface—State equations, molecule areas and covered surface fraction. *Comptes Rendus Acad. Sci. Sér. Iib* **1996**, *323*, 281–289. Available online: <https://api.semanticscholar.org/CorpusID:99056405> (accessed on 10 January 2024).
37. Conder, J.R.; Locke, D.C.; Purnell, J.H. Concurrent solution and adsorption phenomena in chromatography. I. *J. Phys. Chem.* **1969**, *73*, 700–708. [CrossRef]

38. Conder, J.R.; Purnell, J.H. Gas chromatography at finite concentrations. Part 2—A generalized retention theory. *Trans. Faraday Soc.* **1968**, *64*, 3100–3111. [[CrossRef](#)]
39. Conder, J.R.; Purnell, J.H. Gas chromatography at finite concentrations. Part 3—Theory of frontal and elution techniques of thermodynamic measurement. *Trans. Faraday Soc.* **1969**, *65*, 824–838. [[CrossRef](#)]
40. Voelkel, A. Inverse gas chromatography: Characterization of polymers, fibers, modified silicas, and surfactants. *Crit. Rev. Anal. Chem.* **1991**, *22*, 411–439. [[CrossRef](#)]
41. Hamieh, T. New Progress on London Dispersive Energy, Polar Surface Interactions and Lewis's Acid-Base Properties of Solid Surfaces. *Preprints* **2024**, *2024*, 2024010638. [[CrossRef](#)]
42. London, F. The general theory of molecular forces. *Trans. Faraday Soc.* **1937**, *33*, 8–26. [[CrossRef](#)]
43. Gutmann, V. *The Donor-Acceptor Approach to Molecular Interactions*; Plenum: New York, NY, USA, 1978.
44. Riddle, F.L.; Fowkes, F.M. Spectral shifts in acid-base chemistry. Van der Waals contributions to acceptor numbers, Spectral shifts in acid-base chemistry. 1. van der Waals contributions to acceptor numbers. *J. Am. Chem. Soc.* **1990**, *112*, 3259–3264. [[CrossRef](#)]
45. David, R.L. (Ed.) *CRC Handbook of Chemistry and Physics, Internet Version 2007*, 87th ed.; Taylor and Francis: Boca Raton, FL, USA, 2007.
46. Van Oss, C.J.; Good, R.J.; Chaudhury, M.K. Additive and nonadditive surface tension components and the interpretation of contact angles. *Langmuir* **1988**, *4*, 884–891. [[CrossRef](#)]

Disclaimer/Publisher's Note: The statements, opinions and data contained in all publications are solely those of the individual author(s) and contributor(s) and not of MDPI and/or the editor(s). MDPI and/or the editor(s) disclaim responsibility for any injury to people or property resulting from any ideas, methods, instructions or products referred to in the content.